Exact BER computation for cross QAM constellations

Article *in* IEEE Transactions on Wireless Communications · December 2005

DOI: 10.1109/TWC.2005.857997 · Source: IEEE Xplore

3 authors, including:

J.C. Kieffer
University of Minnesota Twin Cities
158 PUBLICATIONS **2,823** CITATIONS

SEE PROFILE

Exact BER Computation for Cross QAM Constellations*

Pavan Kumar Vitthaladevuni, *Member, IEEE*, Mohamed-Slim Alouini, *Senior Member, IEEE*, and John C. Kieffer, *Fellow, IEEE*

***Abstract*—When the number of bits per symbol is odd, the peak and average power of transmission can be reduced by using cross quadrature amplitude modulations (QAMs) instead of rectangular QAMs. However, since perfect Gray coding is not possible for cross QAMs, using Smith-style Gray coding, this paper derives the exact bit error rate (BER) for cross QAM constellations over additive white Gaussian noise (AWGN) and Rayleigh fading channels.**

***Index Terms*—Bit error rate, cross quadrature amplitude modulation, gray penalty, outage probability, rectangular quadrature amplitude modulation, square quadrature amplitude modulation.**

I. Introduction

IT is well known that square quadrature amplitude modulations (QAMs) (i.e., 4-, 16-, 64-, 256-QAMs) are the typically used constellations when the number of bits in a symbol is even. However, when the number of bits per symbol is odd, the rectangular constellation is not a good choice. In [1], Smith shows how both the peak and average power can be reduced by using a cross QAM constellation. Also, it is shown in [1] that there is at least a 1-dB gain in the average signal-to-noise ratio (SNR) by using cross QAMs. As an example, a 32-QAM is shown in Fig. 1 in both rectangular- and cross-shaped constellations.

More recently, cross QAMs have been found to be useful in adaptive modulation schemes wherein the constellation size is adjusted depending on the channel quality. As the channel quality improves, the constellation size $(M = 2^m)$ is increased by incrementing m to $m+1$. If one were to use just square QAMs, the increments should be from m to $m+2$ (for instance, we need to go from 16 to 64 to 256-QAM $\cdots$). Using cross QAMs, however, the increment is smoother (16-QAM to cross 32-QAM to 64-QAM $\cdots$). Since we deal with cross QAMs in this paper, we define $M = 2^{2m+1}$.

Manuscript received March 16, 2004; revised November 2, 2004; accepted November 30, 2004. The editor coordinating the review of this paper and approving it for publication is J. K. Tugnait. This work was supported in part by the Center of Transportation Studies (CTS) through the Intelligent Transportation Systems (ITS) Institute, Minneapolis, MN, and in part by a Doctoral Dissertation Fellowship given by the Graduate School at the University of Minnesota. This paper was presented in part at the 38th Annual Conference on Information Sciences and Systems (CISS 2004), Princeton, NJ, March 2004, and the First International Symposium on Communications, Control and Signal Processing (ISCCSP 2004), Hammamet, Tunisia, March, 2004.

P. K. Vitthaladevuni is with Qualcomm, Inc., San Diego, CA 92121 USA (e-mail: pavan@qualcomm.com).

M.-S. Alouini and J. C. Kieffer are with the Department of Electrical Engineering, University of Minnesota, Minneapolis, MN 55455-0213 USA (e-mail: alouini@ece.umn.edu; kieffer@ece.umn.edu).

Digital Object Identifier 10.1109/TWC.2005.857997

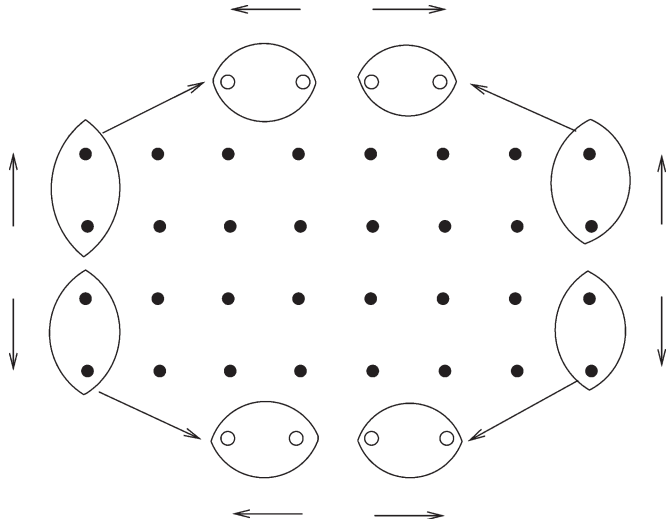

Fig. 1. Construction of a cross 32-QAM from a rectangular 32-QAM. Note the manner in which the points are moved from the sides to the top and bottom.

The remainder of this paper is organized as follows. A systematic way to pseudo-Gray-map cross QAM constellations and approximate performance analysis (both proposed by Smith [1]) will be briefly reviewed in the next section. Section III describes the main differences between the nature of decision boundaries for cross QAMs and those for rectangular QAMs. Section IV introduces a few system parameters. In Section V, we derive exact bit error rate (BER) expressions for each of the $(2m+1)$ bits under additive white Gaussian noise (AWGN) and Rayleigh fading channels. Section VI shows the extension of Smith's approximation to outage probability calculation. Section VII shows the analysis of cross 8-QAMs, which have to be analyzed separately as they do not fall into the same category as the rest of the cross M-QAMs. Finally, Section VIII concludes the paper.

II. Cross M-QAM Construction, Labeling, and Performance ($M \geq 32$)

A. Cross QAM Construction

The cross 32-QAM constellation is constructed as shown in Fig. 1. The black points represent the rectangular 32-QAM. The last columns of symbols on the far left and the far right are moved to the top and bottom rows (white points) in the manner shown (the Gray coding and its modifications are shown in Fig. 2). Similarly, for the cross 128-QAM constellation (Fig. 3), the last two columns on either side are moved (the bottommost

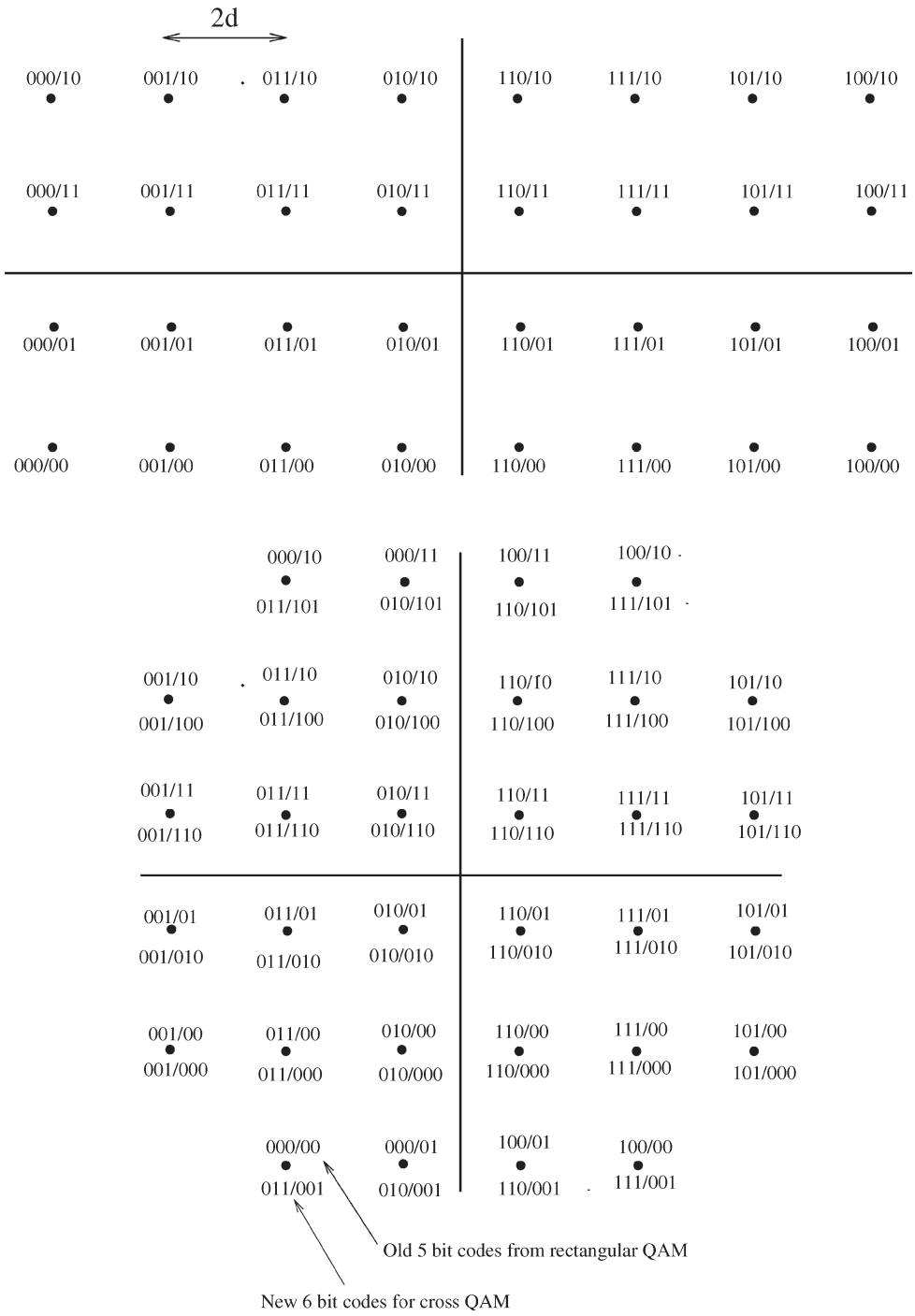

Fig. 2. Rectangular (above) and cross 32-QAM (below) with Gray coding. The 5-bit Gray codes for rectangular and cross QAMs have been written in $i_1i_2i_3/q_1q_2$ fashion. The 6-bit pseudocode generation has also been shown for the cross QAM constellation in the $i_1i_2i_3/q_1q_2q_3$ fashion.

block in the leftmost column becomes the leftmost in the new bottommost column after the move) to the top and bottom in blocks of size 4 in the manner shown. In general, for a cross M-QAM constellation, $\sqrt{2M}/8$ columns from either side are moved to the top and bottom with the arrow spin maintained in the manner shown in Fig. 3.

B. Cross QAM Labeling

Cross QAM labeling has been explained in detail in [1]. For the sake of completeness, we outline the process here. Consider the rectangular QAM constellation. The Gray code and the binary code (in both x- and y-directions) are defined by [2]

$$\begin{aligned} g_j^1 &= b_j^1 \\ g_j^l &= b_j^l \oplus b_j^{l-1},\ 1 \le j \le (2^{m+1} \text{ or } 2^m), \\ & \qquad 1 < l \le (m \text{ or } m+1) \end{aligned} \tag{1}$$

where g_j^l and b_j^l are the lth bits in the Gray and binary codes of the jth symbol. This relation thereby gives a neat transformation for the amplitude of the symbol. However, when

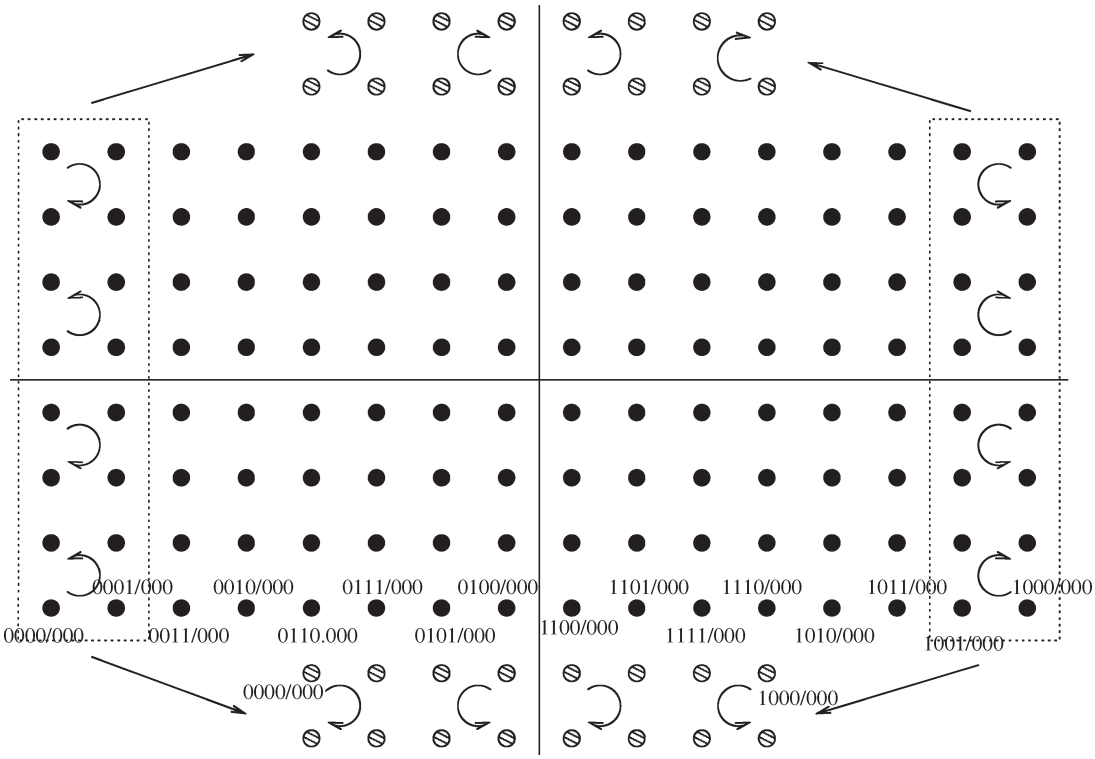

Fig. 3. Construction of a cross 128-QAM from a rectangular 128-QAM. Note the arrow spin through which the points are moved from the sides to the top and bottom.

symbols from the far left and the far right columns are moved to form cross QAM constellation, this relation breaks down. Smith came up with a $(2m+2)$-bit impure Gray code by adding an extra bit in the quadrature phase so as to solve the labeling and modulation problems. Perfect Gray coding is not possible for cross QAM constellations. Note that this extra bit is not transmitted. Its only purpose is to help with the modulation/demodulation. All BER calculations are done with the $(2m+1)$-bit pseudo-Gray code.

Note that in terms of the $(2m+1)$-bit pseudo-Gray code, symbols in the topmost/bottommost row of the original constellation (black points) differ from their nearest newly created white points in exactly two positions: (i_2, q_2) or (i_2, i_3). All other symbols differ from their nearest neighbors by exactly 1 bit. Most importantly, the patterns of change for individual bits in a symbol (except for i_2, q_2 and i_3) along rows or columns of the cross QAM constellation (for example, 10011001 $\cdots$ or 1100001111000011 $\cdots$) are preserved despite the constellation's reshaping. So, the BER expressions of only these 3 bits (i_2, i_3, and q_2) are to be derived separately. BER expressions for all other bits can be deduced easily from the BER expressions for regular pulse-amplitude modulations (PAMs)/QAMs in [2]–[4].

Since the $(2m+1)$-bit Gray codes are imperfect, Smith introduced the concept of Gray penalty G_p as the average number of bits by which two adjacent symbols differ in the constellation [1]. Constellations for which perfect Gray coding is possible have a Gray penalty of 1. The Gray penalty of the cross 32-QAM constellation is 7/6 (there are four symbols with a Gray penalty of 3/2, four with a Gray penalty of 4/3, eight with a Gray penalty of 5/4, and the remaining 16 with a Gray penalty of 1, giving an average of 7/6). For higher cross M-QAMs, G_p can be calculated to be $(1+1/\sqrt{2M}+1/3M)$.[1] Any other type of labeling for cross QAM constellations will result in a higher Gray penalty and as a result a higher BER.

C. Approximate BER Performance

Smith proposed an approximate expression for BER calculation in [1, eq. (7)] that we reproduce as

$$P_b(M) \simeq G_p \frac{N}{\log_2 M} \frac{1}{2} \operatorname{erfc}\left(\frac{d}{\sqrt{N_0}}\right). \tag{2}$$

In this equation, G_p is the Gray penalty, N is the average number of nearest neighbors for a symbol in the constellation [given by $(4-(6/\sqrt{2M}))$ for cross M-QAM[2] when $M \geq 32$], $2d$ is the minimum distance between adjacent symbols in the constellation, and $N_0/2$ is the two-sided noise power spectral density. We shall see in the numerical examples that Smith's approximation is an important expression for the BER.

III. Decision Making at the Receiver ($M \geq 32$)

In the case of rectangular QAM, decision boundaries were quite simple [2]–[4]. The in-phase bits $(i_1 i_2 i_3 \cdots)$ had

[1] In [1], the expression for G_p has a minor typo. The second term appears wrongly as $1/6\gamma$ instead of $1/8\gamma$, with $\gamma = \sqrt{M/32}$.

[2] In [1], the expression for N appears erroneously as $4-(5/8\gamma)$, where $\gamma = \sqrt{M/32}$.

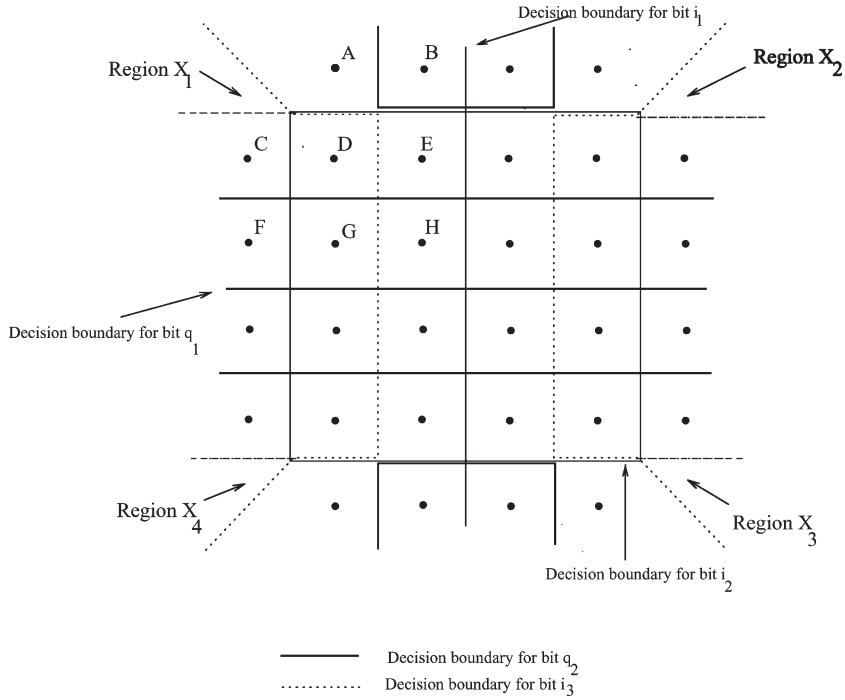

Fig. 4. Decision boundaries for the various bits in cross 32-QAM.

vertical decision boundaries while the quadrature phase bits $(q_1 q_2 q_3 \cdots)$ had horizontal ones. The same is the case for cross M-QAMs if we consider the $(2m+2)$-bit pseudo-Gray codes. We could find out the error probability for each of the $(2m+2)$ bits in the pseudocode and deduce the error for each of the $(2m+1)$ bits in the impure code (which is what we are interested in), as suggested in [1].

Equivalently, for analysis purposes, we could directly analyze the BER of the $(2m+1)$-bit impure Gray code instead of deducing it from the $(2m+2)$-bit pseudocode. However, for the $(2m+1)$-bit cross QAM constellation, due to the fact that symbols are moved from the end columns to the top and bottom of the constellation, the decision boundaries for some bits (i_2, q_2, and i_3) will not be just horizontal or vertical lines. As we shall see, they will be a combination of these.

The decision boundaries for the 5-bit impure Gray code are shown in Fig. 4. Note that for bits i_2, q_2, and i_3, the decision boundaries are a combination of vertical, horizontal, and 45° lines. Fig. 5 deals with cross 128-QAMs and shows that the decision boundaries for bits beyond i_3 (namely, q_3, i_4, ...) are simple straight lines as in the case of regular PAMs/QAMs. Also note that by symmetry, for a cross M-QAM constellation, bits i_1/q_1 have the same BER. Bits i_2, q_2, and i_3 have different BER expressions and are difficult to determine. From then on, the symmetry reappears in the BER of bits q_3/i_4, $q_4/i_5, \ldots, q_m/i_{m+1}$. In contrast, for regular QAMs, bits i_k/q_k have the same BER (for each k).

IV. System Parameters for Cross M-QAM ($M \geq 32$)

In this section, we will define some parameters in order to make our expressions simpler and compact. Note that all the BER expressions will be written in terms of the complementary error (erfc(.)) function whose argument is always a multiple of $d/\sqrt{N_0}$. To save space, we introduce the notation

$$\mathrm{e}_l(i) = \mathrm{erfc}\left(\frac{id}{\sqrt{lN_0}}\right), \quad l = 1, 2, \ldots. \tag{3}$$

On the other hand, it can be easily shown that the average symbol energy E_s for the cross M-QAM constellation is given by

$$\begin{aligned} E_s &= \frac{4}{M}\left[2\left(\frac{3}{4}\sqrt{\frac{M}{2}}\right)\sum_{j=1}^{\frac{3}{4}\sqrt{\frac{M}{2}}}(2j-1)^2 d^2 \right. \\ &\qquad \left. - 2\left(\frac{1}{4}\sqrt{\frac{M}{2}}\right)\sum_{j=1+\frac{1}{2}\sqrt{\frac{M}{2}}}^{\frac{3}{4}\sqrt{\frac{M}{2}}}(2j-1)^2 d^2\right] \\ &= \frac{2}{3}\left(\frac{31M}{32}-1\right)d^2. \end{aligned} \tag{4}$$

Using (4), we can write $d/\sqrt{N_0}$ as

$$\frac{d}{\sqrt{N_0}} = \sqrt{\frac{48}{31M-32}\gamma_s} = \sqrt{\frac{48\log_2 M}{31M-32}\gamma_b} \tag{5}$$

where $\gamma_s = E_s/N_0 = E_b/N_0 \log_2 M = \gamma_b \log_2 M$ is the carrier-to-noise ratio (CNR) at the receiver. Hence, we can leave the BER expressions in terms of $d/\sqrt{N_0}$.

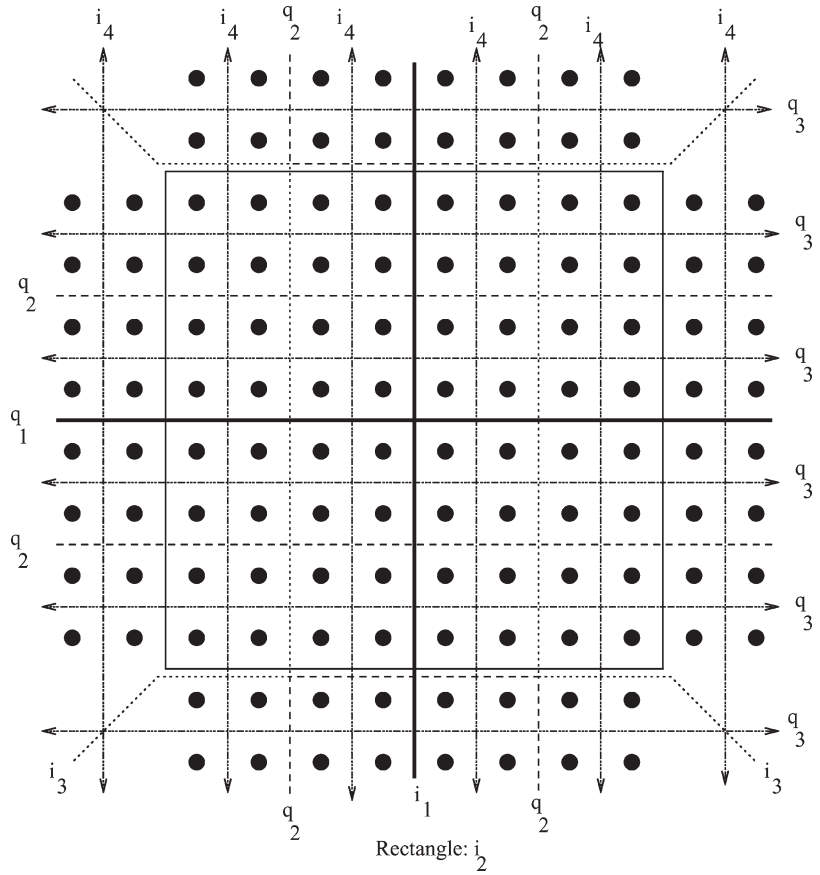

Fig. 5. Decision boundaries for the various bits in cross 128-QAM.

V. BER Expressions for Cross M-QAM ($M \geq 32$)

A. Bits i_1 and q_1

When writing the BER of bit i_1 for a particular symbol (say for symbol "A" in Fig. 4), all we need to look for is the distance between "A" and its decision boundary (y-axis in this case), which is $3d$ in this case. The BER for bit i_1 for symbol "A" can thus be written as

$$P_b(32, i_1|A) = \frac{1}{2}\mathrm{e}_1(3). \tag{6}$$

Note that the BER for bit i_1 is constant along a column, i.e., for symbols A, D, and G; for symbols B, E, and H; and for symbols C and F.

Averaging over all the M symbols (averaging over the symbols of one quadrant is enough due to symmetry) in the cross-QAM constellation, the BER of bit i_1, $P_b(M, i_1)$ can be written as

$$P_b(M, i_1) = \frac{4}{M}\left(p_1(M, i_1) + p_2(M, i_1)\right) \tag{7}$$

where $p_1(M, i_1)$ is the sum of the bit error probabilities for the symbols in the longer central columns and is given by

$$p_1(M, i_1) = \frac{3}{4}\sqrt{\frac{M}{2}} \sum_{i=1}^{\frac{2\sqrt{2M}}{8}} \frac{1}{2}\mathrm{e}_1(2i-1) \tag{8}$$

and $p_2(M, i_1)$ is the sum of the bit error probabilities for the symbols in the short fringe columns and is given by

$$p_2(M, i_1) = \frac{1}{2}\sqrt{\frac{M}{2}} \sum_{i=1+\frac{2\sqrt{2M}}{8}}^{\frac{3\sqrt{2M}}{8}} \frac{1}{2}\mathrm{e}_1(2i-1). \tag{9}$$

Similarly, for bit q_1, the x-axis is the decision boundary, and hence, by symmetry

$$P_b(M, q_1) = P_b(M, i_1). \tag{10}$$

B. Bits q_3, i_4, and Beyond

As pointed out in the section on Gray coding, the BERs of only 3 bits (i_2, q_2, and i_3) are difficult to compute. All others are easily deducible from the original BER expression for PAMs.

For bits q_3 and i_4, the bit pattern along a row/column is of the form 10011001 or 1100001111000011 or 1111000000001111 $\cdots$. Hence, the BER $P_b^c(M, q_3/i_4)$ can be shown to be given by (11) at the bottom of the next page.

For bits q_4/i_5, q_5/i_6, and beyond, the bit pattern along a row/column is the exact opposite of the corresponding pattern for bits i_4/q_3 and is of the form 01100110 or 0011110000111100 or 0000111111110000 $\cdots$. Hence, the BER expression can be easily written as that in (12) at the bottom of the next page.

C. Bit i_2

The decision boundary for bit i_2 is a square centered at the origin and of side length $d\sqrt{2M}$. To compute the BER for this bit, we divide the constellation symbols into two parts: those outside the rectangle and those inside the rectangle. The BER $P_b(M, i_2)$ is given by

$$P_b(M,i_2)=\frac{4}{M}\left[2p_1(M,i_2)p_2(M,i_2)+\left[\frac{M}{8}-(p_2(M,i_2))^2\right]\right] \tag{13}$$

where $2p_1(M,i_2)p_2(M,i_2)$ is the BER for symbols outside the box, $[(M/8)-(p_2(M,i_2))^2]$ is the BER for symbols inside the box, and where $p_1(M,i_2)$ and $p_2(M,i_2)$ are given by

$$p_1(M,i_2)=\sum_{i=1}^{2^{m-2}}\left(\frac{1}{2}\mathrm{e}_1(2i-1)-\frac{1}{2}\mathrm{e}_1(2i-1+2^{m+1})\right) \tag{14}$$

and

$$p_2(M,i_2)=2^{m-1}-\sum_{i=1}^{2^m}\frac{1}{2}\mathrm{e}_1(2i-1). \tag{15}$$

D. Bit q_2

Computation of the BER for bit q_2 gets easier if we divide the BER into two parts: BER due to horizontal decision boundaries $(p_1(M,q_2))$ and BER due to the "U"-shaped and inverted "U"-shaped boundaries $(p_2(M,q_2))$. The BER $P_b^c(M,q_2)$ is given by

$$P_b(M,q_2)=\frac{4}{M}\left(p_1(M,q_2)+p_2(M,q_2)\right) \tag{16}$$

where

$$\begin{aligned}p_1(M,q_2)=&(2^m-2^{m-2})\\&\times\left(\sum_{i=1}^{2^{m-2}}\mathrm{e}_1(2i-1)+\sum_{i=1+2^{m-2}}^{2^{m-1}}\frac{1}{2}\mathrm{e}_1(2i-1)\right.\\&\left.-\sum_{i=1+2^{m-1}}^{3\times2^{m-2}}\frac{1}{2}\mathrm{e}_1(2i-1)\right)+2^{m-2}\\&\times\sum_{i=1}^{2^{m-2}}\left(\frac{1}{2}\mathrm{e}_1(2i-1)-\frac{1}{2}\mathrm{e}_1(2^{m+1}+2i-1)\right)\end{aligned} \tag{17}$$

and

$$\begin{aligned}&p_2(M,q_2)\\&=\left(2^{m-2}-\sum_{i=1}^{2^{m-2}}\left(\frac{1}{2}\mathrm{e}_1(2i-1)-\frac{1}{2}\mathrm{e}_1(2^{m+1}+2i-1)\right)\right)\\&\times\left(\sum_{i=1}^{2^{m-2}}\mathrm{e}_1(2i-1)+\sum_{i=1+2^{m-2}}^{2^{m-1}}\frac{1}{2}\mathrm{e}_1(2i-1)\right.\\&\left.-\sum_{i=1+2^{m-1}}^{3\times2^{m-2}}\frac{1}{2}\mathrm{e}_1(2i-1)\right)\\&+\left(\sum_{i=1}^{2^m}(-1)^{\left\lfloor\frac{i-1}{2^{m-1}}\right\rceil}\frac{1}{2}\mathrm{e}_1(2i-1)\right)\\&\times\left(2^{m-2}-\sum_{i=1+2^{m-1}}^{2^m}\frac{1}{2}\mathrm{e}_1(2i-1)\right).\end{aligned} \tag{18}$$

$$\begin{aligned}P_b\left(M,\frac{q_3}{i_4}\right)=&\sqrt{\frac{2}{M}}\sum_{j=1}^{\sqrt{\frac{M}{32}}}\left[1-g_j^4+\left(2g_j^4-1\right)\left[\sum_{l=1}^{6}\frac{1}{2}(-1)^{l+1}\mathrm{e}_1\left[(2l-1)\frac{\sqrt{2M}}{8}-2j+1\right]\right]\right]\\&+\sqrt{\frac{9}{2M}}\sum_{j=1+\sqrt{\frac{M}{32}}}^{\sqrt{\frac{9M}{32}}}\left[1-g_j^4+\left(2g_j^4-1\right)\left[\sum_{l=1}^{6}\frac{1}{2}(-1)^{l+1}\mathrm{e}_1\left[(2l-1)\frac{\sqrt{2M}}{8}-2j+1\right]\right]\right].\end{aligned} \tag{11}$$

$$\begin{aligned}P_b\left(M,\frac{q_{k-1}}{i_k}\right)=&\sqrt{\frac{2}{M}}\sum_{j=1}^{\sqrt{\frac{M}{32}}}\left[g_j^k+\left(1-2g_j^k\right)\left[\sum_{l=1}^{3\times2^{(k-3)}}\frac{1}{2}(-1)^{l+1}\mathrm{e}_1\left[(2l-1)\sqrt{2M}2^{1-k}-2j+1\right]\right]\right]\\&+\sqrt{\frac{9}{2M}}\sum_{j=1+\sqrt{\frac{M}{32}}}^{\sqrt{\frac{9M}{32}}}\left[g_j^k+\left(1-2g_j^k\right)\left[\sum_{l=1}^{3\times2^{(k-3)}}\frac{1}{2}(-1)^{l+1}\mathrm{e}_1\left[(2l-1)\sqrt{2M}2^{1-k}-2j+1\right]\right]\right].\end{aligned} \tag{12}$$

E. Bit i_3

For bit i_3, the decision regions are slightly more complicated as shown in Fig. 4. The main difference here is to find the probability that a symbol might fall on the wrong side of the 45° lines. Consider the line $x-y=0$. Symbol "H" (in Fig. 4) with coordinates $(-d,d)$ is on the left side of this line, which is basically the side where $x-y<0$. If n_x and n_y represent independent and identically distributed (i.i.d.) AWGN values in the x- and y-directions, then one of the error regions, say region X_2, for bit i_3 in symbol "H" is defined by the region $n_y>3d$ and $-d+n_x-d-n_y>0$. This is the same as $n_y>3d$ and $n_x-n_y>2d$. Since n_x and n_y are zero mean i.i.d. Gaussian random variables, $(n_x-n_y)/\sqrt{2}$ is also Gaussian with zero mean and the same variance as that of n_x and n_y. We divide by $\sqrt{2}$ to make variances the same, so as to make probability computation easier. The correlation coefficient ρ of n_y and $(n_x-n_y)/\sqrt{2}$ is given by

$$\rho=\frac{\mathrm{E}\left(n_y\left(\frac{n_x-n_y}{\sqrt{2}}\right)\right)}{\sigma_{n_y}\sigma_{\frac{n_x-n_y}{\sqrt{2}}}}=-\frac{1}{\sqrt{2}}. \tag{19}$$

Hence, the probability that symbol "H" falls in the error region X_2 can be written using the two-dimensional error function as

$$\frac{1}{4}\,\mathrm{e}_{1,1}\left(3,\frac{2}{\sqrt{2}};-\frac{1}{\sqrt{2}}\right) \tag{20}$$

where

$$\mathrm{e}_{r,s}(i,j;\rho)=\frac{2}{\pi}\int_0^{\phi_1}\exp\left(-\frac{x^2}{\sin^2\theta}\right)\mathrm{d}\theta + \frac{2}{\pi}\int_0^{\phi_2}\exp\left(-\frac{y^2}{\sin^2\theta}\right)\mathrm{d}\theta,\quad x\geq 0, y\geq 0 \tag{21}$$

with

$$\phi_1=\tan^{-1}\left(\frac{\sqrt{1-\rho^2}\frac{x}{y}}{1-\frac{\rho x}{y}}\right)+\frac{\pi}{2}\left(1-\mathrm{sgn}\left(1-\frac{\rho x}{y}\right)\right) \tag{22}$$

$$\phi_2=\tan^{-1}\left(\frac{\sqrt{1-\rho^2}\frac{y}{x}}{1-\frac{\rho y}{x}}\right)+\frac{\pi}{2}\left(1-\mathrm{sgn}\left(1-\frac{\rho y}{x}\right)\right) \tag{23}$$

$$x=i\sqrt{\frac{48(2m+1)}{r(31M-32)}\gamma_b} \tag{24}$$

and

$$y=j\sqrt{\frac{48(2m+1)}{s(31M-32)}\gamma_b}. \tag{25}$$

In this section, i is an odd number, j is an even multiple of $1/\sqrt{2}$, $r=1$, and $s=1$. Also, we will see that the first two arguments to the $e_{r,s}$ function could be negative. In that case, the following identities could be used:

$$\begin{aligned} e_{r,s}(-i,j;\rho)&=2e_s(j)-e_{r,s}(i,j;-\rho)\\ e_{r,s}(i,-j;\rho)&=2e_r(i)-e_{r,s}(i,j;-\rho)\\ e_{r,s}(-i,-j;\rho)&=4-2e_r(i)-2e_s(j)+e_{r,s}(i,j;\rho) \end{aligned} \tag{26}$$

where $e_l(i)$ has already been defined.

The average probability of error $P_b(M,i_3)$ can therefore be written again as a contribution of two components. The first component $[p_1(M,i_3)]$ is the BER due to the horizontal and vertical lines (the rectangular error regions). The second $[p_2(M,i_3)]$ is due to the semi-infinite triangular regions X_1, X_2, X_3, and X_4 (as shown in Fig. 4). Hence, $P_b(M,i_3)$ can be written as

$$P_b(M,i_3)=\frac{4}{M}(p_1(M,i_3)+p_2(M,i_3)) \tag{27}$$

where

$$\begin{aligned} &p_1(M,i_3)\\ &=\left(\sum_{i=1}^{2^{m-1}}\frac{1}{2}\mathrm{e}_1(2i-1)\right)\left(2^{m-1}-\sum_{j=1}^{2^m}\frac{1}{2}\mathrm{e}_1(2j-1)\right)\\ &\quad+\left[\sum_{i=1}^{2^{m-2}}\left(\frac{1}{2}\mathrm{e}_1(2i-1)-\frac{1}{2}\mathrm{e}_1(2i-1+2^{m+1})\right)\right]\\ &\quad\times\left[2^{m-2}+\sum_{j=1}^{2^{m-1}}\frac{1}{2}\mathrm{e}_1(2j-1+2^{m-1})\right]\\ &\quad+2^{m-1}\sum_{i=1}^{2^m}\frac{1}{2}\mathrm{e}_1(2i-1)+\left[2^{m-1}-\sum_{i=1}^{2^m}\frac{1}{2}\mathrm{e}_1(2i-1)\right]\\ &\quad\times\left[\sum_{j=1}^{2^m}(-1)^{\left\lfloor\frac{j-1}{2^{m-1}}\right\rfloor}\frac{1}{2}\mathrm{e}_1(2j-1)\right] \end{aligned} \tag{28}$$

and $p_2(M,i_3)$ is expressed as that shown in (29) at the bottom of the next page.

F. Average BER

Having derived the exact BER of all the bits, the exact average BER for the cross M-QAM constellation $P_b(M)$ can be written as

$$P_b(M)=\frac{1}{2m+1}\left(\sum_{k=1}^{m+1}P_b(M,i_k)+\sum_{k=1}^{m}P_b(M,q_k)\right). \tag{30}$$

As a double check, we have verified our exact BER expressions for various bit positions through Monte Carlo simulations. Fig. 6 shows excellent agreement between the analytical expressions and the simulation results for cross 32- and 128-QAMs.

Fig. 7 compares the exact average BER for the cross 32-, 128-, and 512-QAM constellations with Smith's approximate

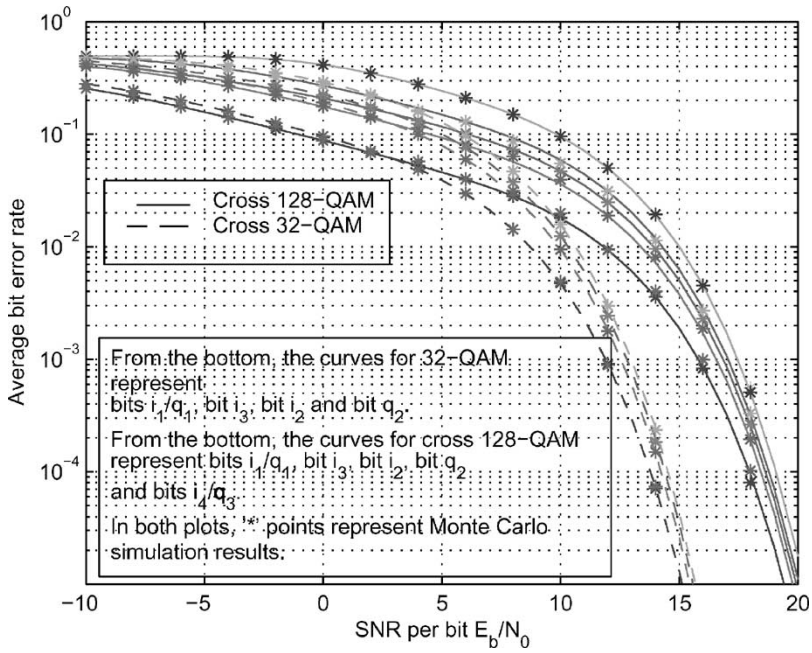

Fig. 6. Comparison of the analytical and simulation results for the average BER of various bits in cross 32-QAM and cross 128-QAM.

BER given in (2). Note that the difference between exact and approximate BER expressions grows as M increases. Note that Smith's expression is a good approximation for cross M-QAMs at high CNRs.

Fig. 8 shows the advantage of using cross-QAMs over rectangular QAMs in adaptive modulations. By using cross-QAMs, we can utilize the extra bit at least 1 dB in advance. In other words, we need a CNR of at least 18 dB at a BER of 10^{-2} to switch over from 16-QAM to rectangular 32-QAM. But, if the system uses cross 32-QAMs, the switch can be made at a CNR of 17 dB.

G. Extension to Rayleigh Fading

Note that all the BER expressions are linear combinations of terms of the form $\mathrm{e}_{r,s}(i,j;\rho)$.[3] To obtain the exact average BER over Rayleigh fading channels, we need to average these terms over the probability density function (pdf) of γ [5, Ch. 2] that is defined by

$$p_\gamma(\gamma) = \frac{1}{\bar{\gamma}}\mathrm{e}^{-\frac{\gamma}{\bar{\gamma}}}, \qquad \gamma > 0 \tag{31}$$

where γ is either γ_b or γ_s. The resultant BER over fading channels is going to be the same linear combination, but of function $\bar{\mathrm{e}}_{r,s}(i,j;\rho)$ in the place of $\mathrm{e}_{r,s}(i,j;\rho)$. $\bar{\mathrm{e}}_{r,s}(i,j;\rho)$ can be shown to be given by

$$\bar{\mathrm{e}}_{r,s}(i,j;\rho) = \frac{2}{\pi}\left[\phi_1+\phi_2-\sqrt{\frac{x^2}{1+x^2}}\tan^{-1}\left(\sqrt{\frac{1+x^2}{x^2}}\tan\phi_1\right)\right.$$
$$\left.-\sqrt{\frac{y^2}{1+y^2}}\tan^{-1}\left(\sqrt{\frac{1+y^2}{y^2}}\tan\phi_2\right)\right], \qquad i,j>0 \tag{32}$$

where ϕ_1, ϕ_2, x, and y have already been defined in (22)–(25), respectively. Again, if the first two arguments of $\mathrm{e}_{r,s}(\cdot,\cdot;\cdot)$ are

[3]Single erfc functions $\mathrm{e}_l(i)$ can be deduced by putting $\rho = 1$ and $j < i$. Products of error functions $\mathrm{e}_r(i)\mathrm{e}_s(j)$ can be deduced by putting $\rho = 0$.

$$p_2(M,i_3) = \sum_{i=1}^{2^m}\sum_{j=1}^{2^{m-1}}\frac{1}{4}\mathrm{e}_{1,1}\left(2i-1,\frac{2^{m-1}-2i+2j}{\sqrt{2}};-\frac{1}{\sqrt{2}}\right)$$
$$+\frac{1}{4}\sum_{i=1}^{2^{m-2}}\sum_{j=1}^{2^m}\left[\mathrm{e}_{1,1}\left(1-2i,\frac{2i+2j-2}{\sqrt{2}};-\frac{1}{\sqrt{2}}\right)+\mathrm{e}_{1,1}\left(2i+2^{m+1}-1,\frac{-2i-2j+2}{\sqrt{2}};-\frac{1}{\sqrt{2}}\right)\right]$$
$$-\frac{1}{4}\sum_{i=1}^{2^m}\sum_{j=1}^{2^{m-1}}\left[\mathrm{e}_{1,1}\left(2i-1,\frac{-2^{m-1}+2j-2i}{\sqrt{2}};-\frac{1}{\sqrt{2}}\right)+\mathrm{e}_{1,1}\left(2i-1,\frac{3\times 2^{m-1}+2j-2i}{\sqrt{2}};-\frac{1}{\sqrt{2}}\right)\right]. \tag{29}$$

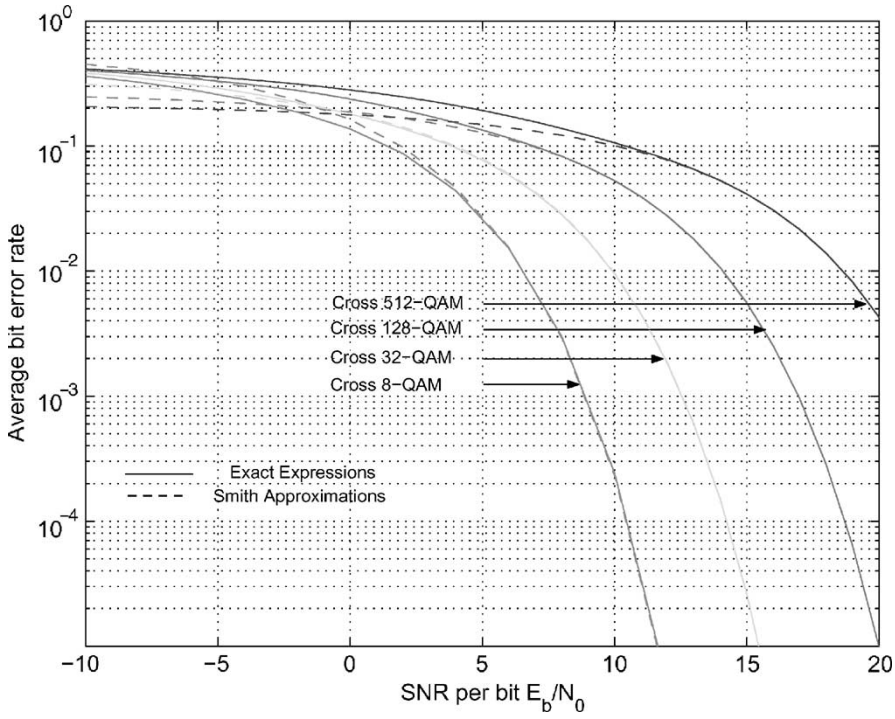

Fig. 7. Comparison between exact and approximate BER expressions for cross 32-, 128-, and 512-QAMs. Note that the difference between exact and approximate expressions increases with an increase in M.

negative, we use the identities

$$\bar{\mathrm{e}}_{r,s}(-i,j;\rho) = \left(1-\sqrt{\frac{y^2}{1+y^2}}\right) - \bar{\mathrm{e}}_{r,s}(i,j;-\rho)$$

$$\bar{\mathrm{e}}_{r,s}(i,-j;\rho) = \left(1-\sqrt{\frac{x^2}{1+x^2}}\right) - \bar{\mathrm{e}}_{r,s}(i,j;-\rho)$$

$$\bar{\mathrm{e}}_{r,s}(-i,-j;\rho) = 4 - \left(1-\sqrt{\frac{x^2}{1+x^2}}\right) - \left(1-\sqrt{\frac{y^2}{1+y^2}}\right) + \bar{\mathrm{e}}_{r,s}(i,j;\rho) \tag{33}$$

where x and y have already been defined in (24) and (25).

Fig. 9 shows the performance of the cross 32-, 128-, and 512-QAMs under Rayleigh fading. Note the more significant difference (compared to the AWGN case) between the exact and approximate expressions when the CNR falls below 5 dB.

VI. Average Bit Error Outage Approximation

It is sometimes of interest to evaluate the average BER outage (defined as the probability that the BER, averaged over fading, fails to meet a target BER [6]). Due to the reasonable accuracy of Smith's approximation (as shown in Fig. 9), it can be used to evaluate the average BER outage probability. For convenience, we reproduce Smith's approximation under AWGN as

$$P_b(E) \simeq G_p \frac{N}{\log_2 M}\frac{1}{2}\mathrm{erfc}\left(\frac{d}{\sqrt{N_0}}\right) = G_p \frac{N}{\log_2 M}\frac{1}{2}\mathrm{erfc}\left(\sqrt{\frac{48\log_2 M}{31M-32}\gamma_b}\right). \tag{34}$$

Averaging (34) over Rayleigh fading leads to

$$\overline{P}_b(E) \simeq G_p \frac{N}{\log_2 M}\frac{1}{2}\left(1-\sqrt{\frac{48\overline{\gamma}_b\log_2 M}{31M-32+48\overline{\gamma}_b\log_2 M}}\right). \tag{35}$$

Hence, for a given target average BER $\overline{P}_b^*(E)$, we can invert this expression to get the approximate target average SNR per bit ($\overline{\gamma}_b^*$) to be

$$\overline{\gamma}_b^* \simeq \frac{(31M-32)\left(\frac{G_pN}{2\log_2 M}-\overline{P}_b^*(E)\right)^2}{48\log_2 M\left(\frac{G_pN\overline{P}_b^*(E)}{\log_2 M}-\overline{P}_b^{*2}(E)\right)}. \tag{36}$$

We experience an average BER outage when the average BER falls below the target BER $\overline{P}_b^*(E)$ or equivalently when the SNR per bit $\overline{\gamma}_b$ falls below $\overline{\gamma}_b^*$. This outage probability can be calculated using the fact that the average SNR per bit $\overline{\gamma}_b$ has a log-normal pdf given by

$$p_{\overline{\gamma}_b}(\xi) = \frac{10}{\sqrt{2\pi}\xi\sigma_{\mathrm{dB}}\ln(10)}\exp\left(-\frac{(10\log_{10}(\xi)-\mu_{\mathrm{dB}})^2}{2\sigma_{\mathrm{dB}}^2}\right) \tag{37}$$

where μ_{dB} and σ_{dB}^2 are the mean and the variance of the Gaussian random variable $10\log_{10}\overline{\gamma}_b$. Hence, the outage probability P_o can be written using the well known cumulative distribution function of the log-normal random variable as

$$P_o = \frac{1}{2}\mathrm{erfc}\left(\frac{\mu_{\mathrm{dB}}-10\log(\overline{\gamma}_b^*)}{\sigma_{\mathrm{dB}}\sqrt{2}}\right). \tag{38}$$

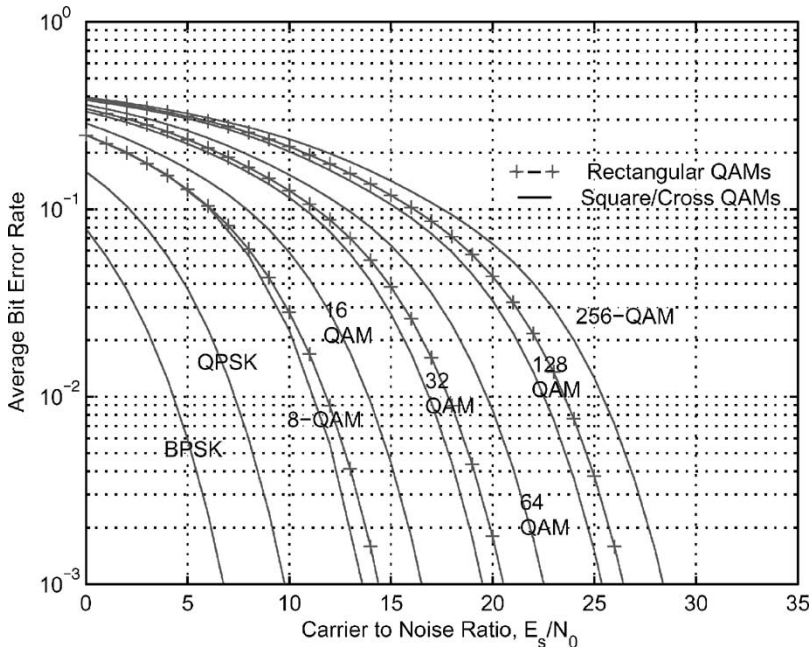

Fig. 8. Advantage of using cross QAMs. Additional bit can be used at least 1 dB in advance.

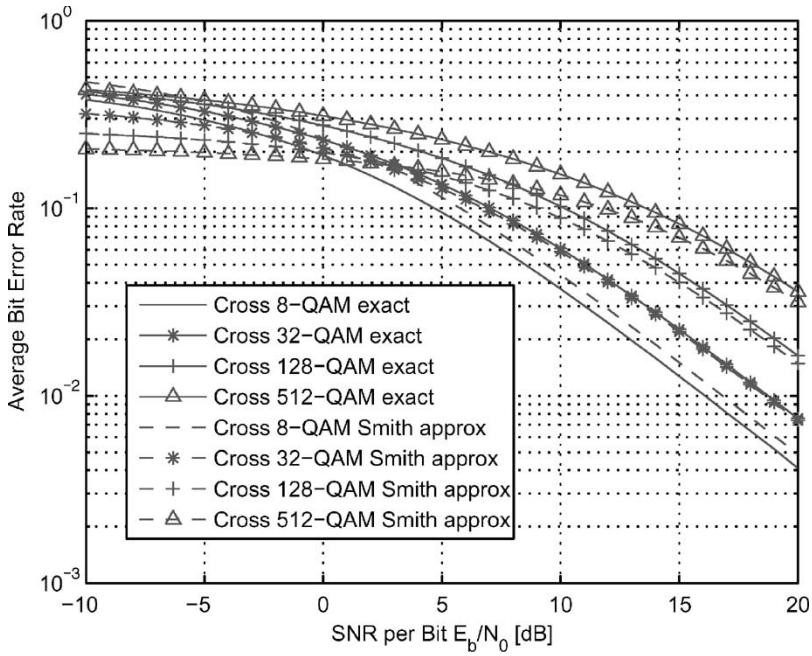

Fig. 9. Average BER of cross M-QAM under Rayleigh fading.

Fig. 10 shows the approximate BER outage probability as a function of the target average BER for cross 32-, 128-, and 512-QAMs. Note the excellent agreement between the analytical and the simulation results for 32-, 128-, and 512-QAMs.

VII. Cross 8-QAM

Cross 8-QAMs do not strictly fall into the same category as the rest of the cross QAMs. Perfect Gray coding is not possible for this configuration. However, since the cross 8-QAM constellation has only eight symbols, we found the best pseudo-Gray coding scheme (that which minimizes G_p) through exhaustive search. Fig. 11 shows a cross 8-QAM constellation along with its decision boundaries.

The symbol error rate for cross 8-QAMs [also known as (4, 4) constellations] has been derived in [7] using Craig's approach [8]. The exact BER expressions for this constellation can also be written using Craig's approach. However, in this

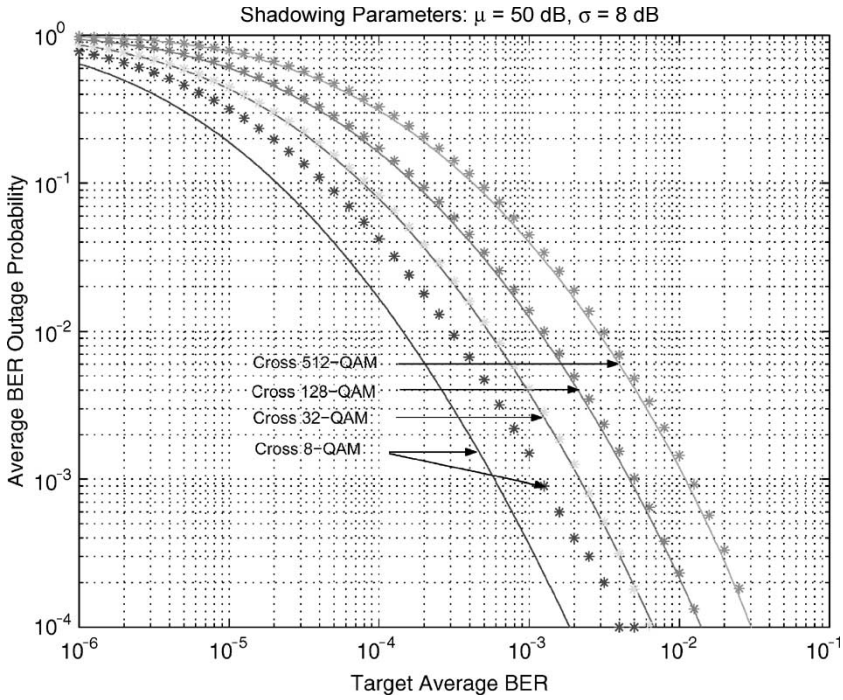

Fig. 10. Approximate outage probability as a function of average bit error probability under Rayleigh fading.

paper, we present the exact BER expressions in terms of the two-dimensional erfc(·) function

$$\begin{aligned}P_b(8,i_1) &= P_b(8,q_1)\\ &= \frac{1}{16}\Big[\mathrm{e}_{1,1}(-1,1;-0.5)+\mathrm{e}_{1,1}(1,-\sqrt{3};0.5)\\ &\quad+\mathrm{e}_{1,1}(0,1;0.5)+\mathrm{e}_{1,1}(0,2+\sqrt{3};-0.5)\\ &\quad+\mathrm{e}_{1,1}(1,0;0.5)+\mathrm{e}_{1,1}(-1,1+\sqrt{3};-0.5)\\ &\quad+\mathrm{e}_{1,1}(-1-\sqrt{3},1+\sqrt{3};-0.5)\\ &\quad+\mathrm{e}_{1,1}(1+\sqrt{3},0;0.5)\Big]\\ P_b(8,i_2) &= \frac{1}{4}+\frac{1}{8}\Big[2\mathrm{e}_{1,1}(1,-1;0)+\mathrm{e}_{1,1}(-1,1;-0.5)\\ &\quad+\mathrm{e}_{1,1}(1,\sqrt{3};-0.5)\\ &\quad+\mathrm{e}_{1,1}(1+\sqrt{3},0;-0.5)\\ &\quad+\mathrm{e}_{1,1}(-1-\sqrt{3},1+\sqrt{3};-0.5)\\ &\quad-\mathrm{e}_{1,1}(-1,1+\sqrt{3};-0.5)\\ &\quad-\mathrm{e}_{1,1}(1,0;-0.5)-\mathrm{e}_{1,1}(0,-1;-0.5)\\ &\quad-\mathrm{e}_{1,1}(0,2+\sqrt{3};-0.5)\Big]. \end{aligned} \tag{39}$$

Smith's approximate expression in (2) can be extended to this case ($G_p = 10/8$, $N = 3$) giving

$$P_b \simeq \frac{10}{16}\mathrm{erfc}\left(\frac{d}{\sqrt{N_0}}\right). \tag{40}$$

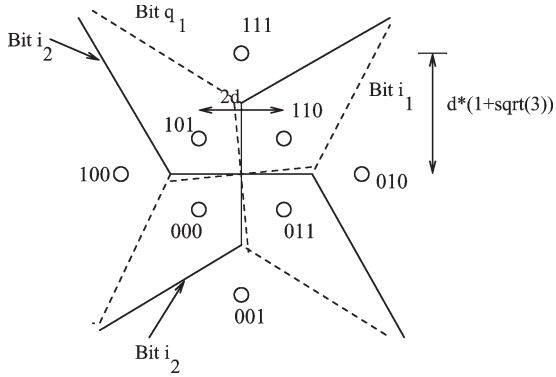

Fig. 11. Decision boundaries for the various bits in cross 8-QAM.

Again, as in Section VI, the average outage probability P_o [for a given target average bit error probability $\overline{P}_b^*(E)$] can be easily shown to be given by

$$P_o = \frac{1}{2}\mathrm{erfc}\left(\frac{\mu_{\mathrm{dB}} - 10\log(\overline{\gamma}_b^*)}{\sigma_{\mathrm{dB}}\sqrt{2}}\right) \tag{41}$$

where

$$\overline{\gamma}_b^* \simeq \frac{\sqrt{3}\left(1-1.6\overline{P}_b^*(E)\right)^2}{(1+\sqrt{3})\left(3.2\overline{P}_b^*(E)-\left(1.6\overline{P}_b^*(E)\right)^2\right)}. \tag{42}$$

Fig. 7 compares the exact average BER for cross 8-QAMs with Smith's approximate BER given in (2). Note that Smith's expression is an upper bound for cross 8-QAM while it is not so for the others. This is because cross 8-QAMs do not strictly fall under the category of cross M-QAMs. Fig. 9 compares Smith's approximation with the exact analytical expression for cross 8-QAMs under Rayleigh fading. Note the significantly larger

gap between approximation and exact expression. Once again, this is because cross 8-QAMs do not strictly fall under the category of cross M-QAMs. Fig. 10 shows the approximate BER outage probability as a function of the target average BER for cross 8-QAM. Note that the approximation is not very good here. Once again, this is because cross 8-QAM does not fall into the same category as the rest of the cross QAMs. Hence, Smith's approximation is not as accurate as it is for the rest of cross QAMs.

VIII. Conclusion

In this paper, we have derived exact and generic closed-form expressions for the BER of cross M-QAM constellations under Smith-style pseudo-Gray coding. We have compared the exact BER expressions with Smith's approximation and have found that Smith's approximation is a simple and close approximation, especially for high CNR values, over AWGN channels. As a corollary, we have also used Smith's expressions to approximate the BER outage probability for cross M-QAMs.

References

[1] J. G. Smith, "Odd-bit quadrature amplitude shift keying," *IEEE Trans. Commun.*, vol. COMM-23, no. 3, pp. 385–389, Mar. 1975.

[2] P. K. Vitthaladevuni and M.-S. Alouini, "A recursive algorithm for the exact BER computation of generalized hierarchical QAM constellations," *IEEE. Trans. Inf. Theory*, vol. 49, no. 1, pp. 297–307, Jan. 2003.

[3] K. Cho and D. Yoon, "On the general BER expression of one and two dimensional amplitude modulations," *IEEE Trans. Commun.*, vol. 50, no. 7, pp. 1074–1080, Jul. 2002.

[4] P. K. Vitthaladevuni and M.-S. Alouini, "A closed-form expression for the exact BER of generalized PAM and QAM constellations," *IEEE Trans. Commun.*, vol. 52, no. 5, pp. 698–700, May 2004.

[5] M. K. Simon and M.-S. Alouini, *Digital Communications Over Fading Channels*, 2nd ed. New York: Wiley, Nov. 2002.

[6] A. Conti, M. Z. Win, M. Chiani, and J. H. Winters, "Bit error outage for diversity reception in shadowing environment," *IEEE Commun. Lett.*, vol. 7, no. 1, pp. 15–17, Jan. 2003.

[7] X. Dong, N. C. Beaulieu, and P. H. Wittke, "Signaling constellations for fading channels," *IEEE Trans. Commun.*, vol. COMM-47, no. 5, pp. 703–714, May 1999.

[8] J. W. Craig, "A new, simple, and exact result for calculating the probability of error for two-dimensional signal constellations," in *Proc. IEEE Military Communications Conf. (MILCOM)*, McLean, VA, Oct. 1991, pp. 571–575.

Pavan Kumar Vitthaladevuni (S'00–M'04) received the B.Tech. degree in electrical engineering from the Indian Institute of Technology (IIT), Madras, India, in 1999 and the M.S.E.E and Ph.D. degrees from the University of Minnesota, Twin Cities, Minneapolis, MN, in 2001 and 2004, respectively.

During the summers of 2002 and 2003, he was an intern at Texas Instruments, Inc., San Diego, CA, where he worked on improving packet detection algorithms and spur-removal filters for the IEEE 802.11 (wireless local area network, WLAN) receiver. He is currently a Senior Engineer at Qualcomm Inc., San Diego, CA. His research interests span digital communications over wireless channels and information theory.

Mohamed-Slim Alouini (S'94–M'98–SM'03) was born in Tunis, Tunisia. He received the Ph.D. degree in electrical engineering from the California Institute of Technology (Caltech), Pasadena, CA, in 1998.

In September 1998, he joined the Department of Electrical and Computer Engineering, University of Minnesota, Minneapolis, MN, where he is currently an Associate Professor. His current research interests lie in the area of performance analysis of wireless communication systems.

John C. Kieffer (M'86–SM'87–F'93) was born and raised in St. Louis, MO. He received the Ph.D. degree in mathematics from the University of Illinois Urbana-Champaign, Urbana, in 1970.

From 1970 to 1986, he held regular academic appointments at the University of Missouri, Rolla, and in 1986 at the University of Minnesota Twin Cities, Minneapolis, MN, where he is currently a Professor at the Department of Electrical and Computer Engineering. He has held visiting positions at Stanford University from 1978 to 1979, at the University of Illinois Urbana-Champaign in 1980 and from 1984 to 1985, at the University of Arizona from 1996 to 1997 and in 2001, and at the Swiss Federal Institute of Technology (ETH) Zurich in 1997. His principal research area involves information theory.